Tumor and Stem Cell Biology

Cancer Research

The Polycomb Group Protein Bmi-1 Is Essential for the Growth of Multiple Myeloma Cells

Zainab Jagani, Dmitri Wiederschain, Alice Loo, Dan He, Rebecca Mosher, Paul Fordjour, John Monahan, Michael Morrissey, Yung-Mae Yao, Christoph Lengauer, Markus Warmuth, William R. Sellers, and Marion Dorsch

Abstract

Bmi-1 is a member of the Polycomb group family of proteins that function in the epigenetic silencing of genes governing self-renewal, differentiation, and proliferation. Bmi-1 was first identified through its ability to accelerate c-Myc–induced lymphomagenesis. Subsequent studies have further supported an oncogenic role for Bmi-1 in several cancers including those of the breast, lung, prostate, and brain. Using a stable and inducible shRNA system to silence Bmi-1 gene expression, we show a novel role for Bmi-1 in regulating the growth and clonogenic capacity of multiple myeloma cells both *in vitro* and *in vivo*. Moreover, to elucidate novel gene targets controlled by Bmi-1, global transcriptional profiling studies were performed in the setting of induced loss of Bmi-1 function. We found that the expression of the proapoptotic gene Bim is negatively regulated by Bmi-1 and that Bim knockdown functionally rescues the apoptotic phenotype induced upon loss of Bmi-1. Therefore, these studies not only highlight Bmi-1 as a cancer-dependent factor in multiple myeloma, but also elucidate a novel antiapoptotic mechanism for Bmi-1 function involving the suppression of Bim. *Cancer Res; 70(13); 5528–38. ©2010 AACR.*

Introduction

Bmi-1 was initially discovered through its ability to cooperate with c-Myc in the induction of lymphoma (1, 2) and was subsequently recognized as a member of the Polycomb group (PcG) family of proteins (3). The PcG proteins function within distinct multisubunit complexes and epigenetically regulate gene expression by altering chromatin states at specific promoters (reviewed in Schwartz and colleagues in ref. 4). In several contexts, including lymphoma, mouse embryonic fibroblasts, and human fibroblasts, Bmi-1 exerts its oncogenic function, at least in part, by silencing the *INK4a/ARF* (*Cdkn2a*) tumor suppressor locus encoding the p16 (INK4a) and p19 (ADP ribosylation factor, ARF) proteins (5–7). The proposed role for Bmi-1 as a key regulator of cell growth control/senescence mechanisms led to additional investigations about the role of Bmi-1 in tumorigenesis. Several studies have shown that Bmi-1 is overexpressed in medulloblastomas (8), lung (9), breast (10), prostate cancers (11), and multiple myeloma (MM; ref. 12–14), among others. Extensive microarray analyses of multiple cancer types also indicate that a distinct Bmi-1–driven gene expression signature is a predictor of metastasis and poor survival (15, 16). A functional contribution of Bmi-1 in tumorigenesis has been reported in several cancers (17–20), yet the precise mechanism(s) by which it promotes cell growth, especially in cases that are independent of *INK4a/ARF* suppression, have yet to be elucidated (19, 21). Mouse models of Bmi-1 deficiency have also established the importance of Bmi-1 in the self-renewal of neural and hematopoietic stem cells (8, 22–24). In concordance with its role in stem cells, Bmi-1 has been proposed to maintain cancer stem cell populations in leukemia (22), as well as in breast (25) and lung cancers (17).

Although analysis of published gene expression profiling data reveals an increase in Bmi-1 expression in MM patient samples and cell lines compared with normal plasma cells in three independent studies (12–14), the precise role of Bmi-1 in the growth of MM cells remains unknown and is therefore the focus of this study. In addition, the contribution of epigenetic mechanisms toward the pathogenesis of MM is not well understood. MM is a genetically heterogeneous and complex malignancy characterized by the abnormal proliferation of antibody-producing plasma cells (reviewed in Seidl and colleagues in ref. 26). Although current therapies including proteasome inhibitors, thalidomide, and lenalidomide have met with some success, the disease is still incurable (27).

In this study, we investigate whether Bmi-1 is necessary for the growth of MM cells both *in vitro* and *in vivo*. We not only delineate a contribution of this PcG protein in MM cell growth but also determine a novel mechanism by which Bmi-1 promotes survival. Transcriptional profiling studies in the RPMI-8226 myeloma cell line followed by functional

Authors' Affiliation: Novartis Institutes for BioMedical Research, Cambridge, Massachusetts

Note: Supplementary data for this article are available at Cancer Research Online (http://cancerres.aacrjournals.org/).

Current address for C. Lengauer: Sanofi-Aventis, 13 Quai Jules Guesde 94403 Vitry-sur-Seine, France.

Corresponding Author: Marion Dorsch, 250 Massachusetts Avenue, Cambridge, MA 02139. Phone: 617-871-3942; Fax: 617-871-4083; E-mail: marion.dorsch@novartis.com.

doi: 10.1158/0008-5472.CAN-09-4229

rescue experiments showed that the proapoptotic gene Bim is negatively regulated by Bmi-1, and that this regulation is required for the Bmi-1–mediated inhibition of apoptosis in these cells. Overall, these studies highlight the importance of epigenetic mechanisms, as contributed by Bmi-1 function, toward the survival of MM cells.

Materials and Methods

Cell culture

RPMI-8226, NCI-H929, and U266 myeloma cells were obtained from the American Type Culture Collection. KMS12BM, LP-1, OPM-2, and EJM lines were obtained from the German Resource Centre for Biological Material. All cell lines were maintained in advanced RPMI-8226 medium (Invitrogen) with 1% fetal bovine serum, and 1% L-Glutamine.

Short hairpin RNA constructs

Control short hairpin RNA (shRNA): GTGGACTCTTGAAAGTACTAT, Bmi-1 shRNA-1: CCAGACCACTACTGAATATAA (TRCN0000020155), and Bmi-1 shRNA-2: CCTAATACTTTCCAGATTGAT (TRCN000 0020156) were cloned into the inducible pLKO-Tet-On puromycin vector as previously described (28). The Bim shRNA sequence (29) was cloned into the pLKO-Tet-On neomycin vector.

Lentivirus and infection

Lentiviral supernatants were generated according to our previously established protocol (28) and concentrated by ultracentrifugation followed by infection of MM cells as described in the Supplementary Methods.

Cell lysates, immunoblotting, and antibodies

Snap-frozen cell pellets of primary $CD138^+$ plasma cells isolated from the bone marrow of healthy donors were purchased from Stem Cell Technologies. Cells were harvested in lysis buffer (Cell Signaling). Anti–Bmi-1 Clone F6 was from Millipore; anti–glyceraldehyde-3-phosphate dehydrogenase was from Imgenex; anti-TetR was from Boca Scientific; anti–β-actin was from Sigma; anti-cleaved poly ADP ribose polymerase (PARP) and anti–caspase-3 were from Cell Signaling Technology; and anti-Bim was from Thermoscientific.

RNA extraction and quantitative reverse transcription-PCR

Total RNA was isolated using the RNeasy Mini kit (Qiagen) or the TurboCapture 96 mRNA isolation kit (Qiagen). RNA samples were processed for quantitative reverse transcription-PCR (qRT-PCR) as previously described (30).

Clonogenic, cell cycle/apoptosis assays

Two thousand to 8,000 cells per well were seeded in a 48-well plate in methycellulose medium (HSC-001; Stem Cell Technologies). A stock of 1.44% methylcellulose was made in medium and diluted to a final concentration of 1.17% by the addition of cell suspension. Colonies were stained with Hoechst 33342 after 14 days and visualized using the ChemGenius imaging system. Colony number and area were analyzed using the AlphaEase FC program [AlphaInnotech (Cell Biosciences)]. Cell cycle analysis was performed using the CycleTEST PLUS DNA Reagent kit (Becton Dickinson), whereas apoptotic cells were detected using the Annexin V-FITC/7-AAD kit (BD Biosciences).

Transcriptional profiling

RNA was isolated using the Qiagen RNeasy mini kit (Qiagen). Generation of labeled cDNA and hybridization to HG-U133 Plus2 arrays (Affymetrix) were performed as previously described (20). Expression values were normalized on a per-sample basis using the Affymetrix MAS5 algorithm (31). Microarray expression data have been deposited in Gene Expression Omnibus (accession number GSE 21912).

Animals

Female nonobese diabetic severe combined immunodeficient mice (Charles River Laboratories) were allowed to acclimate in the Novartis Institutes for BioMedical Research animal facility with *ad libitum* access to food and water for at least 3 days before manipulation. Animals were handled in accordance with the Novartis Animal Care and Use Committee protocols and regulations.

Efficacy study of doxycycline-inducible Bmi-1 shRNA

Stably infected RPMI-8226 cells were free of *Mycoplasma* and viral contamination (comprehensive mitogen-activated protein panel, RADIL, University of Missouri). Mice (ages 6–8 wk) were inoculated s.c. with 8×10^6 cells in 50% Matrigel (BD Biosciences) in the right dorsal axillary region. Tumor dimensions were obtained using calipers, and tumor volume was calculated as (length × width^2)/2. Two to three weeks after implantation, animals were randomized and sorted into treatment groups (n = 10) based on tumor volume (mean = 140 mm^3). Animals received vehicle (5% sucrose) or doxycycline (Sigma Aldrich; 1 mg/mL in 5% sucrose) via drinking water for the duration of the study (27 d).

Immunohistochemical staining

Tumor samples were fixed in 10% neutral-buffered formalin for 6 hours and processed using the Ventana Discovery System (CC1S_ R60_NH _OR) and as described in Supplementary Methods.

Chromatin immunoprecipitation

RPMI-8226 cells were treated with or without doxycycline for 48 hours, and cross-linking/chromatin immunoprecipitation (ChIP) was performed as described in Supplementary Methods. Antibodies used include the Rabbit IgG control (SC-2027 Santa Cruz Biotech) and a Bmi-1 polyclonal antibody generously provided by Drs. Caroline Woo and Robert Kingston (Massachusetts General Hospital, Boston, MA). DNA obtained after ChIP was analyzed through qPCR using SYBR green with oligos specific for the Bim promoter, and enrichments were calculated by normalizing to input DNA

(see Supplementary Methods for primer sequences and calculation methods).

Statistical analyses

All data are shown as mean values ± SD and tested statistically using the two-tailed Student's *t* test. $P \leq 0.05$ was considered to indicate statistical significance. *In vivo* tumor measurement data are shown as mean ± SEM and was tested statistically using the Kruskal Wallis One way ANOVA and the *post hoc* Dunn's method for pairwise comparisons. $P < 0.05$ was considered to indicate statistical significance.

Results

Bmi-1 is required for the clonogenic growth of MM cells

We first examined the status of Bmi-1 protein expression in a panel of MM cell lines. Whole-cell extracts were subjected to immunoblot detection of Bmi-1, and the presence of Bmi-1 protein was verified in all MM cell lines that were tested. (Fig. 1A). Bmi-1 protein was also detected at higher levels in MM cell lines than in the normal donor derived $CD138^+$ plasma cells that were analyzed (Fig. 1A). Interestingly, Bmi-1 migrated with distinct mobilities in certain cell lines (compare KMS12BM to RPMI-8226), raising the possibility that there is differential posttranslational modification of Bmi-1. To ensure that such species represent Bmi-1, immunoblots were also prepared in cell lines with and without Bmi-1 shRNA–mediated knockdown, and indeed, these protein species were each attenuated upon Bmi-1 knockdown (Supplementary Fig. S1C and E; Fig. 1B). To determine whether Bmi-1 protein was required for MM cell growth, we infected RPMI-8226, KMS12BM, and LP1 cells with a robust inducible single-lentiviral vector knockdown reagent pLKO-Tet-On (28) containing either control nontargeting shRNA or two distinct Bmi-1–targeting shRNA sequences (Bmi-1 shRNA-1 or Bmi-1 shRNA-2), and polyclonal stable lines were obtained after puromycin selection. Doxycycline induction of Bmi-1 shRNAs but not the control nontargeting shRNA led to the significant reduction of Bmi-1 mRNA (Supplementary Fig. S1A) and protein (Fig. 1B), which was more pronounced with Bmi-1 shRNA-1 than with Bmi-1 shRNA-2. To determine the effect of Bmi-1 knockdown on MM cell growth and viability, stable lines were grown in the presence or absence of doxycycline and the number of viable cells was determined using an MTS-assay. Doxycycline induction of both Bmi-1 shRNAs in RPMI-8226 cells correlated with >60% inhibition of cell growth over a time course of 7 days (Fig. 1C). Bmi-1 knockdown in KMS12BM and LP1 cells also led to the inhibition of cell proliferation but was less extensive and slightly delayed compared with RPMI-8226 cells (Supplementary Fig. S2A and B). To determine whether Bmi-1 was required for the clonogenic growth of MM cells, cells were plated in methylcellulose in the presence or absence of doxycycline. In this case, we observed that Bmi-1 knockdown led to the inhibition of colony formation by causing a reduction in colony number rather than size in all the three myeloma lines, RPMI-8226, KMS12BM (Fig. 2; Supplementary Fig. S3), and LP1 (Supplementary Fig. S4). Therefore, taken together, these results strongly suggest that Bmi-1 plays a necessary role in the *in vitro* growth of MM cells.

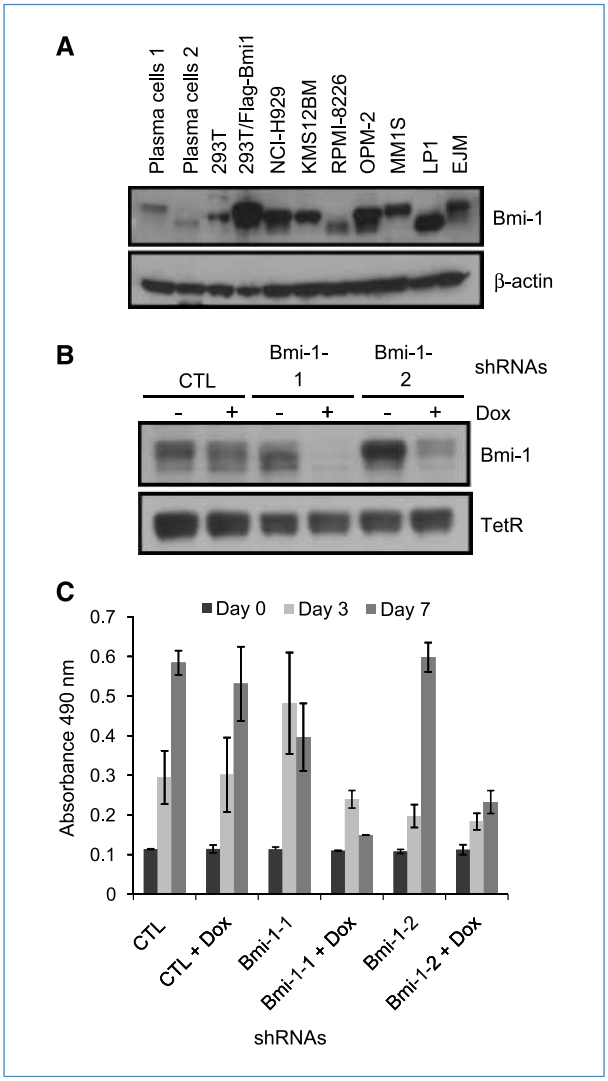

Figure 1. shRNA-mediated knockdown of Bmi-1 inhibits the growth of MM cells. A, immunoblot confirming the expression of Bmi-1 in MM cell lines. Lysates of $CD138^+$ bone marrow–derived plasma cells from two unique healthy donors are also included. Flag-tagged Bmi-1 expressed in 293T cells is used as a positive control, and β-actin serves as a loading control. B, immunoblot showing reduction of Bmi-1 protein upon doxycycline (dox) treatment (72 h, 100 ng/mL) of RPMI-8226 cells stably transduced with inducible Bmi-1 shRNA-1 or Bmi-1 shRNA-2. A nontargeting control (CTL) shRNA was included. Tetracycline Repressor (TetR) expression is included as a control and indicates the presence of the inducible shRNA lentiviral vector. C, control or Bmi-1 shRNA-RPMI-8226 cells were seeded at 1,000 to 2,000 cells per well in a 96-well plate in triplicate. Cells were treated with doxycycline, and cell growth was measured using the Cell Titer 96 Aqueous One Solution cell proliferation assay at the indicated times. Experiments shown are representative of at least three independent experiments and $P < 0.05$ for doxycycline induction of both Bmi-1 shRNAs compared with uninduced controls at 7 d of doxycycline treatment.

Bmi-1 inhibits apoptosis in MM cells

In several cellular contexts, Bmi-1 has been shown to promote cell cycle progression, and counteract senescence and apoptosis by silencing the expression of $p16^{INK4a}$ and $p19^{ARF}$ tumor suppressors (5, 6). To determine the mechanism by which Bmi-1 regulates the growth of MM cells, we stained cellular DNA with propidium iodide, allowing examination of the various phases of the cell cycle by flow cytometry during the loss of Bmi-1 function. Doxycycline induction of RPMI-8226 cells containing Bmi-1 shRNA led to a prominent appearance of a sub-G_1 DNA content peak indicative of a population that has undergone cell death (Fig. 3A). The proportion of dead cells continued to increase through day 6 (Fig. 3B) and day 9 after doxycycline induction by which time >60% of cells showed sub-G_1 DNA content (Supplementary Fig. S5). To further confirm whether RPMI-8226 cells with Bmi-1 depletion undergo apoptotic cell death, cells were stained with FITC-labeled Annexin V. Induction of Bmi-1 shRNAs led to a statistically significant ($P < 0.005$) 15% to 30% increase in cells exclusively staining with Annexin V after 3 days of doxycycline treatment (Fig. 3C; Supplementary Fig. S12), indicating that this population is undergoing the early stages of apoptosis. Bmi-1 depletion in KMS12BM and LP1 cells did not significantly alter their cell cycle profile but yielded the detection of a 20% and 7% sub-G_1 DNA content, respectively, suggesting that only a proportion of these cells undergo cell death (Supplementary Fig. S6). Therefore, the induction of cell death partially explains the pronounced inhibition of colony formation observed in KMS12BM and LP1 cells upon Bmi-1 knockdown and leaves the possibility of additional mechanisms such as cellular senescence. Overall, these data show that although the apoptotic response upon Bmi-1 depletion varies among MM cell lines suggestive of multiple Bmi-1–driven growth mechanisms, they clearly define a function for Bmi-1 in protecting RPMI-8226 myeloma cells from apoptosis.

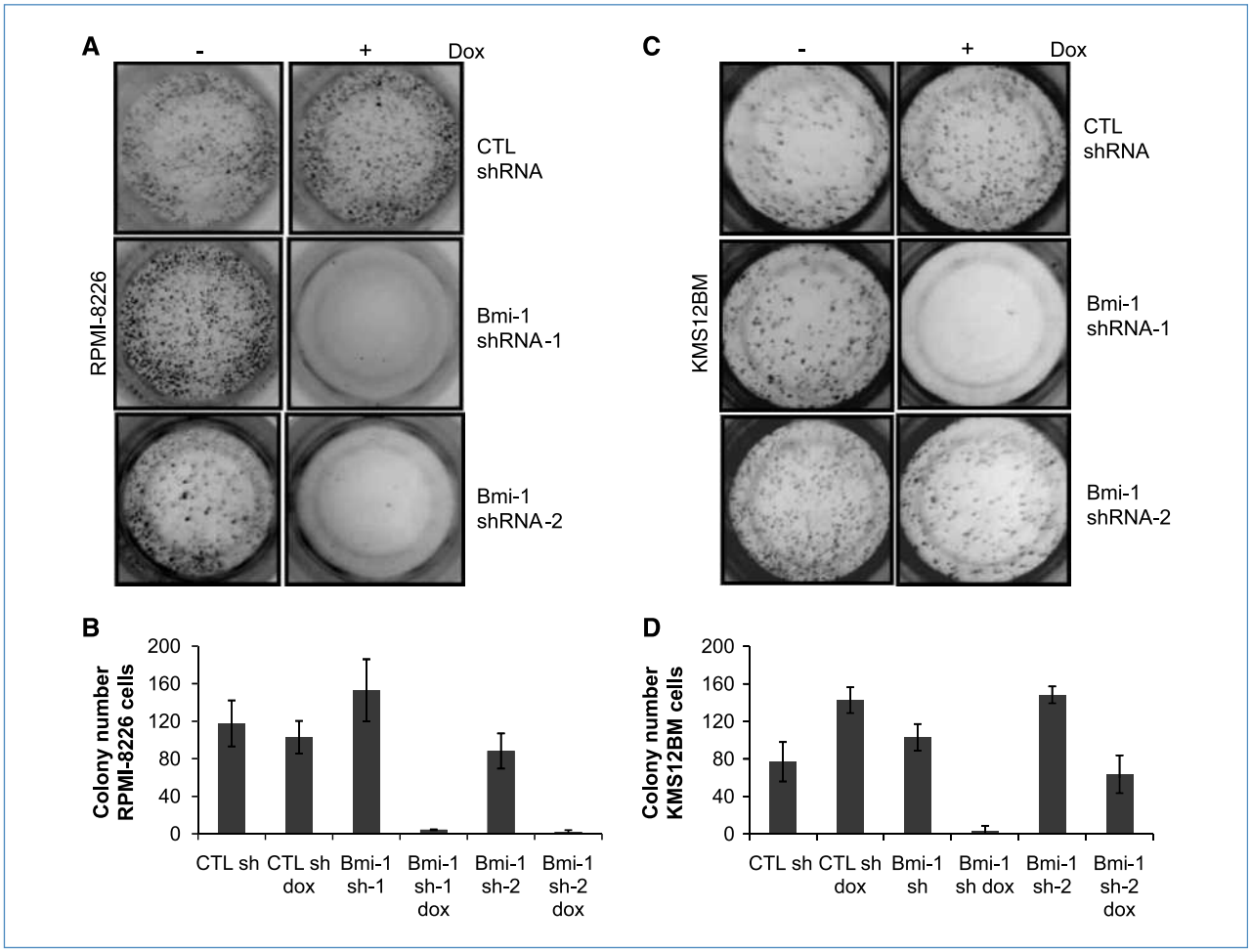

Figure 2. shRNA-mediated knockdown of Bmi-1 inhibits the clonogenic capacity of MM cells. Bmi-1 shRNA or control shRNA containing RPMI-8226 (A) and KMS12BM cells (C) were grown in methylcellulose in the presence or absence of doxycycline for 14 d (triplicate), after which colonies were visualized by Hoechst 33342 staining. Images were captured using the ChemiGenius Bioimaging system, and a representative well from each condition is shown. B and D, quantitative analysis of colony formation in (B) RPMI-8226 cells and (D) KMS12BM cells, showing significant reduction ($P < 0.05$) in colony number upon doxycycline induction of both Bmi-1 shRNAs.

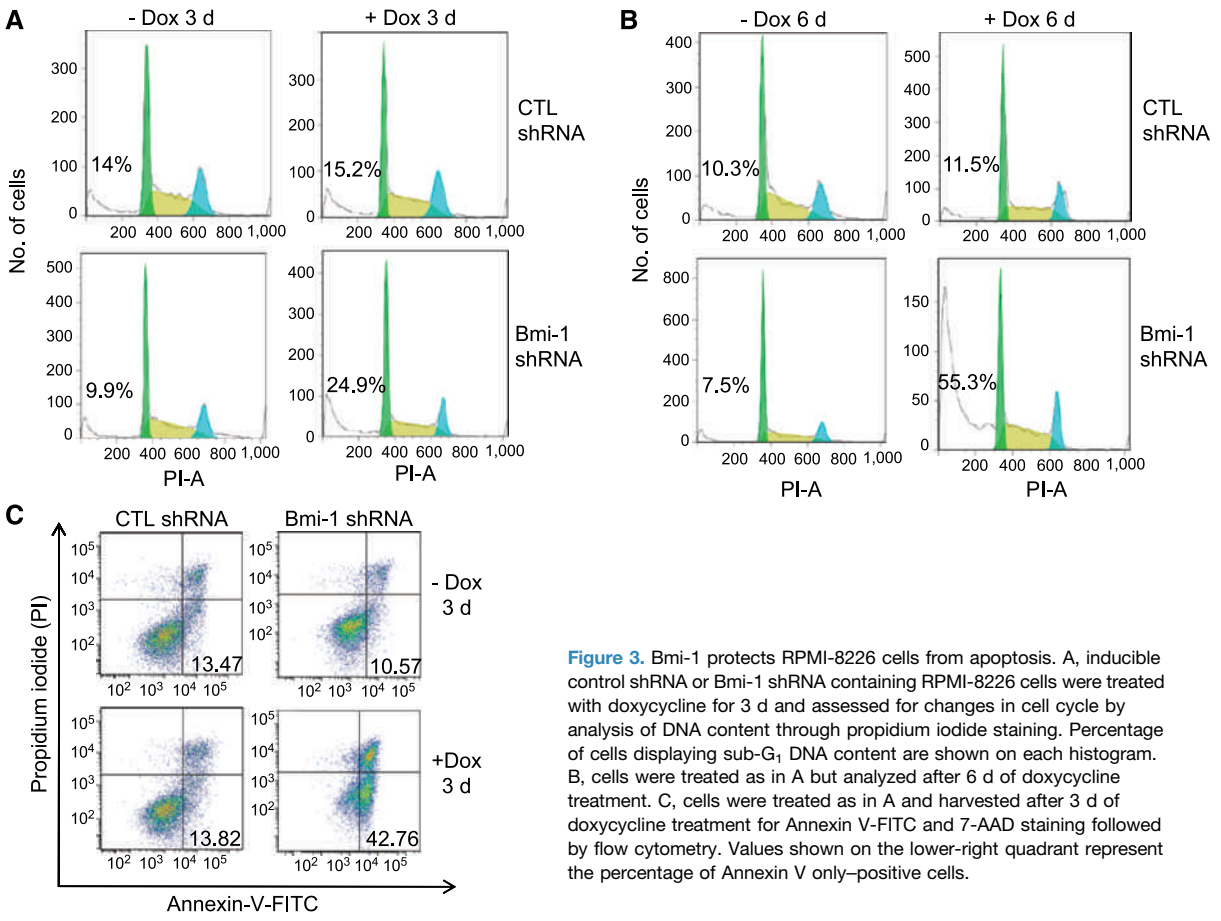

Figure 3. Bmi-1 protects RPMI-8226 cells from apoptosis. A, inducible control shRNA or Bmi-1 shRNA containing RPMI-8226 cells were treated with doxycycline for 3 d and assessed for changes in cell cycle by analysis of DNA content through propidium iodide staining. Percentage of cells displaying sub-G_1 DNA content are shown on each histogram. B, cells were treated as in A but analyzed after 6 d of doxycycline treatment. C, cells were treated as in A and harvested after 3 d of doxycycline treatment for Annexin V-FITC and 7-AAD staining followed by flow cytometry. Values shown on the lower-right quadrant represent the percentage of Annexin V only–positive cells.

Bmi-1 is necessary for the growth of RPMI-8226 cells *in vivo*

To determine whether Bmi-1 is also necessary for MM cell growth *in vivo*, we generated subcutaneous MM xenografts in nonobese diabetic severe combined immunodeficient mice using the inducible control shRNA and Bmi-1 shRNA-RPMI-8226 cells. To confirm that the doxycycline treatment led to inhibition of Bmi-1 expression, we analyzed a separate group of animals 4 days after doxycycline treatment. Doxycycline induction of Bmi-1 shRNAs led to 96% inhibition of Bmi-1 mRNA, as measured by qRT-PCR (Fig. 4A), and depletion of Bmi-1 protein (Fig. 4B). Knockdown of Bmi-1 was stable and persisted throughout the 27-day treatment period (Supplementary Fig. S7). In contrast to vehicle treatments and doxycycline-treated control shRNA tumors, doxycycline-treated animals bearing Bmi-1 shRNA RPMI-8226 xenografts showed a marked inhibition of overall tumor growth (Fig. 4C). Furthermore, in keeping with the notion that Bmi-1 might function as a prosurvival factor, we observed that Bmi-1–depleted tumors began to regress at day 5 of doxycycline treatment, displaying an average 70% regression by day 23. In agreement with the apoptotic phenotype observed upon Bmi-1 knockdown *in vitro*, immunohistochemical staining revealed a marked increase in cleaved caspase-3 in doxycycline-treated Bmi-1 shRNA cells compared with vehicle-treated animals (Fig. 4D). Quantitative analysis of the immunohistochemical data using a pixel-counting algorithm[1] also indicated an average 2.8-fold increase in cleaved caspase-3 signal in doxycycline-treated ($n = 6$) over vehicle-treated ($n = 3$) Bmi-1 shRNA tumor xenografts (Supplementary Fig. S8). Therefore, these results provide *in vivo* evidence for a role of Bmi-1 in the growth and survival of RPMI-8226 cells.

Transcriptional profiling reveals novel Bmi-1–regulated genes

Emerging evidence indicates that Bmi-1 also functions in an INK4a/ARF-independent manner in the normal as well as in the tumorigenic context, yet the precise targets involved have not been elucidated (19, 21). Bmi-1 knockdown neither resulted in the restoration of *p16* nor an increase in *p14* (human *ARF*) mRNAs in all three myeloma lines (RPMI-8226, LP1, and

[1] J. Deeds, unpublished.

KMS12BM) tested (data not shown). Given the profound anti-apoptotic effect of Bmi-1 in RPMI-8226 cells, we took advantage of our inducible Bmi-1 shRNA system to dissect the signaling that occurs downstream of Bmi-1 in these cells. HG-U133 Plus2 Affymetrix gene chips were used to analyze global changes in gene expression resulting from Bmi-1 knockdown. Because a significant reduction of Bmi-1 protein was detected beginning 24 hours after doxycycline treatment (Fig. 5A), transcriptional profiling was performed during doxycycline-mediated Bmi-1 shRNA induction at 24, 32, and 48 hours collecting data from biological triplicates at each time point.

To minimize the effect of doxycycline treatment alone or of the control shRNA vector alone in the data analysis, we grouped all the 33 "control" samples (biological triplicates of Bmi-1 shRNA without doxycycline; control shRNA with and without doxycycline at 24, 32, and 48 h, and Bmi-1 shRNA and control shRNA before doxycycline treatment). The 9 Bmi-1 shRNA + doxycycline samples (24, 32, and 48 h, in biological triplicates) were grouped together and were compared through the two-tailed Student's t test to the control sample group described above. Table 1 shows genes that were differentially regulated in response to Bmi-1 knockdown. False discovery rates were calculated

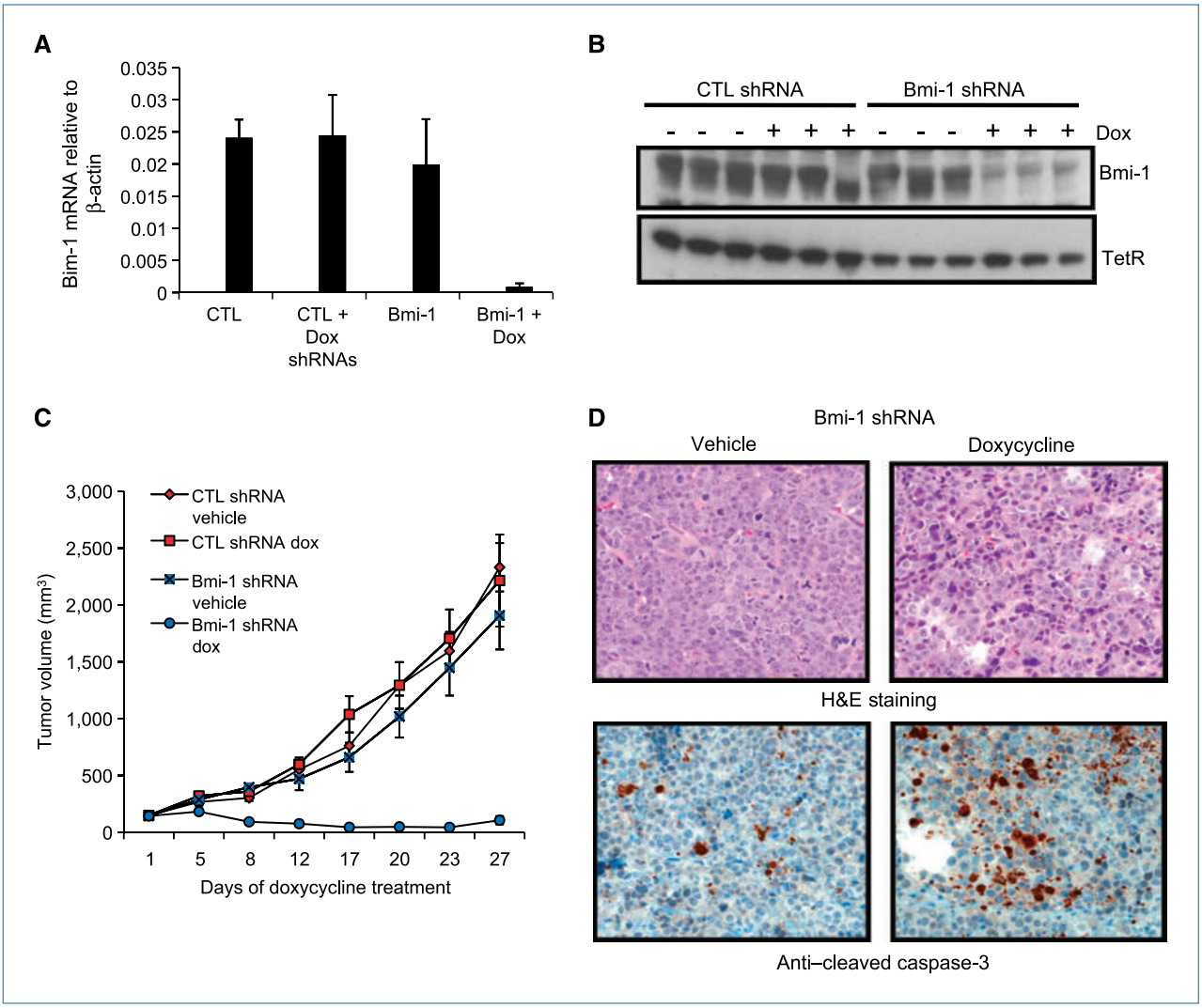

Figure 4. Bmi-1 is necessary for MM tumor growth *in vivo*. A, qRT-PCR of Bmi-1 mRNA transcripts in inducible Bmi-1 shRNA or control shRNA RPMI-8226 xenografts. Tumors were harvested 4 d after the start of doxycycline (1 mg/mL) or vehicle (5% Sucrose) treatment. Columns, mean from three tumors within each treatment group; bars, SD. $P < 0.005$ for Bmi-1 shRNA with doxycycline compared with Bmi-1 shRNA (vehicle). B, immunoblot indicating knockdown of Bmi-1 protein in tumors harvested 4 d after the start of vehicle or doxycycline treatments. C, control and Bmi-1 shRNA xenografts were analyzed for tumor growth during a time course of doxycycline or vehicle treatment. Tumor volume is reported as mean ± SEM. $n = 10$ per treatment group. One way ANOVA (with *post hoc* Dunn's method pairwise comparisons) yielded $P < 0.05$ for the Bmi-1 shRNA doxycycline group compared with Bmi-1 shRNA vehicle, control shRNA vehicle, and control shRNA doxycycline groups. D, tumors harvested at the end of the study (27 d) were fixed in formalin and subsequently processed for H&E staining, as well as immunohistochemical staining for cleaved caspase-3. Images (×200 magnification) were acquired using the Aperio image scanscope.

using the Benjamini-Hochberg step-down method (32). Fold changes were modest, ranging between 1.5 and 2 for genes most consistently upregulated, and 1.5 to 6 for genes consistently repressed, but were highly significant. The two-tailed student *t* test and false discovery rate calculation was also performed for each time point of doxycycline induction (Supplementary Table S1).

Interestingly, several genes that were found to be upregulated upon Bmi-1 depletion, such as *Bcl2l11* (*Bim*), *P115, GAS2,* and *FAM26B,* have been linked to apoptosis (33–36). Among these genes, Bim has well-defined roles in the execution of apoptosis (33, 37). Our analysis also revealed genes that were repressed upon Bmi-1 knockdown, suggesting that Bmi-1 may function directly or indirectly in maintaining the expression of such genes. Indeed, the most highly repressed gene in the doxycycline-treated Bmi-1 shRNA group was Bmi-1, therefore validating a crucial factor in this experiment. In agreement with the induction of proapoptotic genes upon Bmi-1 silencing, repression of the antiapoptotic gene, *apoptosis inhibitor-5/AAC-11*(*API5*; Supplementary Fig. S9D; Table 1; ref. 38) was observed. The changes in gene expression for several genes from the microarray analysis, including *Bim, API-5*, and *MAPK6*, were reconfirmed in the original RNA samples by parallel qRT-PCR analysis (Supplementary Fig. S9). In summary, global transcriptional profiling led to the identification of several potential downstream mediators of Bmi-1 function in myeloma cells, most notably a group of apoptosis regulators.

Bmi-1 regulates the expression of the proapoptotic gene *Bim*

The finding that the expression of the proapoptotic gene Bim is upregulated upon Bmi-1 knockdown in RPMI-8226 cells is in accordance with the prominent apoptotic phenotype that is detected in these cells and reveals a novel potential target downstream of Bmi-1. We further investigated this regulation *in vitro* and *in vivo*. In a similar time course experiment to that performed for the transcriptional profiling studies, a gradual increase in Bim mRNA was detected from 16 to 72 hours postdoxycycline induction of Bmi-1 shRNA (Fig. 5A), thereby corroborating the results from the microarray experiment. A maximal 1.6-fold increase was detected 32 hours after doxycycline induction, a time point at which Bmi-1 protein is significantly reduced (Fig. 5A). Therefore, these data indicate a correlation between the loss of Bmi-1 protein and an increase in *Bim* mRNA transcript levels. Immunoblots of doxycycline-treated Bmi-1 shRNA-RPMI-8226 cells also indicated an increase in Bim protein, in particular the Bim L and Bim s isoforms, upon Bmi-1 knockdown (Fig. 5B). Although the changes in Bim mRNA and protein seem modest, previous studies have shown that minor changes in Bim expression are sufficient to confer functional effects (39–41). The regulation of Bim was also observed *in vivo*, wherein Bim protein increased 4 days after doxycycline treatment of Bmi-1 shRNA-RPMI-8226–transplanted animals (Fig. 5C). Taken together, these data suggest that Bmi-1 can regulate Bim both *in vitro* and *in vivo*. We next determined whether a potential mechanism by which Bmi-1 controls Bim expression is through the regulation at the Bim promoter. We performed ChIP studies in RPMI-8226 cells using a Bmi-1–specific antibody previously used for ChIP (42). Although detection of Bmi-1 binding at the *Bim* promoter varied through the 2,500-bp region upstream of the transcriptional start site (TSS), it was highest at ~700 bp upstream from the TSS as determined by

Table 1. Genes significantly upregulated or downregulated upon Bmi-1 knockdown

Gene symbol	*t* test (Bmi-1 shRNA + Dox vs controls, pooled time points)	Genes upregulated (fold change)	Gene symbol	*t* test (Bmi-1 shRNA + Dox vs controls, pooled time points)	Genes downregulated (fold change)
BCL2L11	9.2E-12	1.53	*SLC39A10*	1.59E-25	0.46
BCL2L11	6.27E-10	1.57	*SFXN1*	1.16E-24	0.26
SERPINH1	9.71E-09	1.64	*MAPK6*	1.69E-24	0.42
HGF	1.22E-08	1.52	*MRPL10*	4.08E-24	0.48
PI15	1.28E-08	1.80	*API5*	1.16E-23	0.42
C1orf173	8.16E-08	1.81	*SFXN1*	2.50E-23	0.30
FZD3	1.14E-07	1.51	*UQCRB*	2.51E-23	0.35
FAM26B	1.43E-07	1.66	***BMI-1***	1.66E-22	0.17
GAS2	1.67E-07	1.99	*EIF4G2*	1.03E-20	0.57
TLE1	3.17E-07	1.68	*DONSON*	4.63E-20	0.59
SMOX	3.63E-07	1.55	*DCUN1D5*	1.70E-19	0.64
PLAGL2	3.76E-07	1.55	*GMFB*	7.69E-19	0.55
CD38	4.36E-07	1.69	*PDIA4*	2.49E-18	0.58
MGC34646	4.81E-07	1.74	*LOC285636*	6.74E-18	0.56
			TWF1	1.89E-17	0.48
			ISCU	2.71E-17	0.61

NOTE: Genes are ranked by FDR significance and filtered for fold changes >1.5 and <0.67.

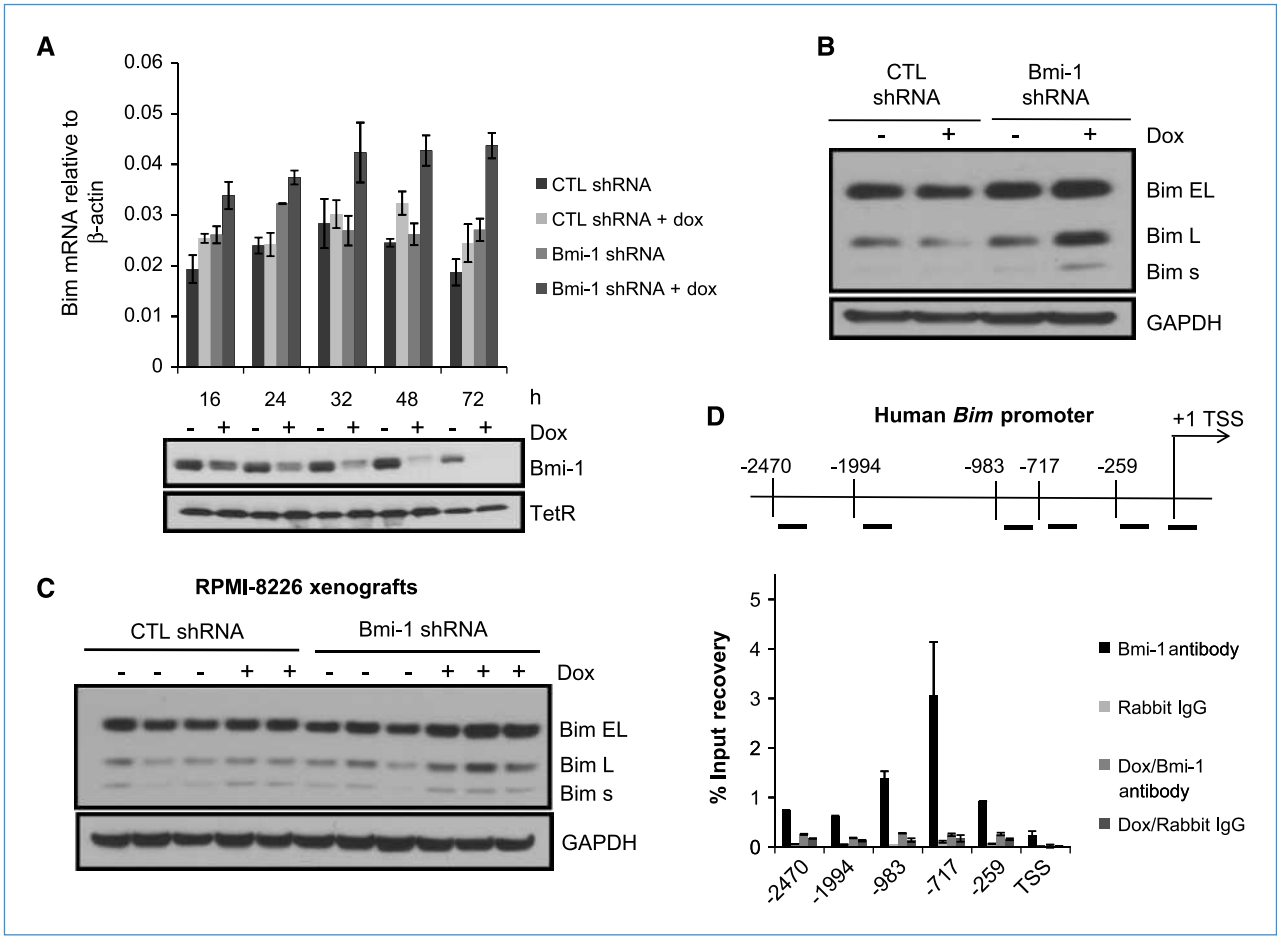

Figure 5. Bim mRNA and protein are increased upon Bmi-1 knockdown. A, qRT-PCR showing relative levels of Bim mRNA through a time course of doxycycline induction of control shRNA or Bmi-1 shRNA-RPMI-8226 cells. Each experiment was performed in triplicate and repeated at least thrice, and $P < 0.05$ at 48 and 72 h postdoxycycline induction of Bmi-1 shRNAs. Below is an immunoblot showing reduction of Bmi-1 protein through the time course of doxycycline induction. B, immunoblot showing an increase in Bim protein upon doxycycline treatment (72 h) of Bmi-1 shRNA-RPMI-8226 cells. GAPDH, glyceraldehyde-3-phosphate dehydrogenase. C, immunoblot showing an increase in Bim protein (Bim EL and L isoforms) in doxycycline-treated (4 d) Bmi-1shRNA-RPMI-8226 xenografts. D, a schematic of the human *Bim* promoter showing locations of primer sets (amplifying 100- to 120-bp regions) relative to the TSS. Below is the corresponding ChIP qPCR data showing % input recovery from these regions within the *Bim* promoter in ChIP samples from nontreated or doxycycline-treated RPMI-8226 cells that were subjected to either the Bmi-1 antibody or control rabbit IgG antibodies. Bmi-1 binding is highest ~700-bp upstream from the TSS. Points, mean from duplicate samples; bars, SEM.

quantitative PCR (Fig. 5D). Importantly, cells that were treated with doxycycline to induce Bmi-1 shRNAs failed to show enrichment at such loci within the Bim promoter (Fig. 5D), confirming that the observed interaction was dependent on Bmi-1. Therefore, these studies suggest that Bmi-1 regulates *Bim* expression through interaction at the Bim promoter.

Bmi-1–mediated suppression of Bim is important for the inhibition of apoptosis

To determine the functional significance of Bim upregulation upon Bmi-1 knockdown, we generated RPMI-8226 cells containing inducible expression of both Bmi-1 and Bim shRNAs. We hypothesized that if suppression of Bim plays an important role for Bmi-1–imposed cell survival, the depletion of Bim should rescue cells from undergoing apoptosis upon Bmi-1 knockdown. Doxycycline induction of Bim shRNA led to a decrease in Bim mRNA as measured by qRT-PCR (Fig. 6A). Importantly, doxycycline induction of Bim shRNA was sufficient to block the increase in Bim mRNA levels that is otherwise detected upon Bmi-1 knockdown alone (Fig. 6A). Bmi-1 was efficiently depleted in doxycycline-induced Bmi-1shRNA and Bmi-1shRNA/Bim shRNA cells (Fig. 6B). Furthermore, doxycycline induction of control shRNA/Bim shRNA and Bmi-1shRNA/Bim shRNA cells resulted in a significant decrease of Bim protein (Fig. 6B). Additionally, although cleaved PARP, a well-established marker of apoptosis, was upregulated upon Bmi-1 knockdown, this increase was not detected in the presence of simultaneous Bmi-1 and Bim knockdown (Fig. 6B). Therefore, these results show that Bim knockdown is sufficient to negatively affect known markers of apoptosis (Fig. 6B). In agreement with the attenuation of cleaved PARP observed upon dual Bmi-1/Bim knockdown and in sharp contrast to the inhibition of cell growth observed upon Bmi1 knockdown, simultaneous knockdown of Bim

and Bmi-1 resulted in a phenotypic rescue with ~80% of the cells surviving Bmi-1 depletion as long as 8 days after doxycycline induction (Fig. 6C). We confirmed the rescue observed upon dual Bmi-1/Bim knockdown in clonogenic assays (Supplementary Fig. S10) and Annexin V apoptosis assays (Supplementary Fig. S11) with both Bmi-1 shRNAs. Quantitation of colony formation (Supplementary Fig. S10B) and Annexin V staining (Supplementary Fig. S12) confirmed statistically significant differences ($P < 0.05$) between induction of Bmi-1 shRNA alone compared with induction of both Bmi-1 and Bim shRNAs. These results show that the regulation of Bim by Bmi-1 is an important mechanism by which Bmi-1 inhibits apoptosis in RPMI-8226 cells.

Discussion

Although MM represents a malignancy in which several genetic and tumor microenvironment factors have been proposed to promote the tumorigenic phenotype (43, 44), the contribution of epigenetic mechanisms toward this disease is not clearly understood. The PcG proteins, of which Bmi-1 is a critical member, serve evolutionarily conserved functions in epigenetic gene regulation during development, with emerging evidence implicating their role in tumorigenesis (45). For example, in keeping with its ability to accelerate lymphoma in E-μ-Myc mice, Bmi-1 overexpression can also cause lymphoma in the E-μ-Bmi-1 transgenic model (1, 2, 46). In addition, Bmi-1 can immortalize mouse embryonic fibroblasts as well as cooperate with oncogenic RAS to transform fibroblasts and mammary epithelial cells (6, 47, 48). Here, we show, using an inducible shRNA system, that Bmi-1 is essential for the maintenance of the transformed phenotype of myeloma cells both *in vitro* and *in vivo*. As a core constituent of the Polycomb-repressive complex 1, Bmi-1 stimulates the Histone H2A ubiquitin ligase activity of Polycomb-repressive complex 1, thereby maintaining silencing that is initiated by the Polycomb-repressive 2 complex (reviewed in ref. 45). In future studies, it will be interesting to interrogate the relative contribution of Bmi-1 versus the other PcG proteins in MM as well as the mechanisms leading to their constitutive expression. Several possibilities exist since previous studies have shown that c-MYC can induce Bmi-1 expression (49), and c-MYC is highly expressed in MM lines including the ones analyzed in this study.

A well-established and extensively studied mechanism by which Bmi-1 promotes tumorigenesis is through the transcriptional silencing of the *p16* and *p19* tumor suppressor genes (5, 6). Whereas p16 inhibits cell cycle progression by disrupting the cyclinD/CDK4/6 complex, p19 inhibits Mdm2 function resulting in p53 stabilization and subsequent apoptosis. In particular, by inhibiting p19, Bmi-1 is able to

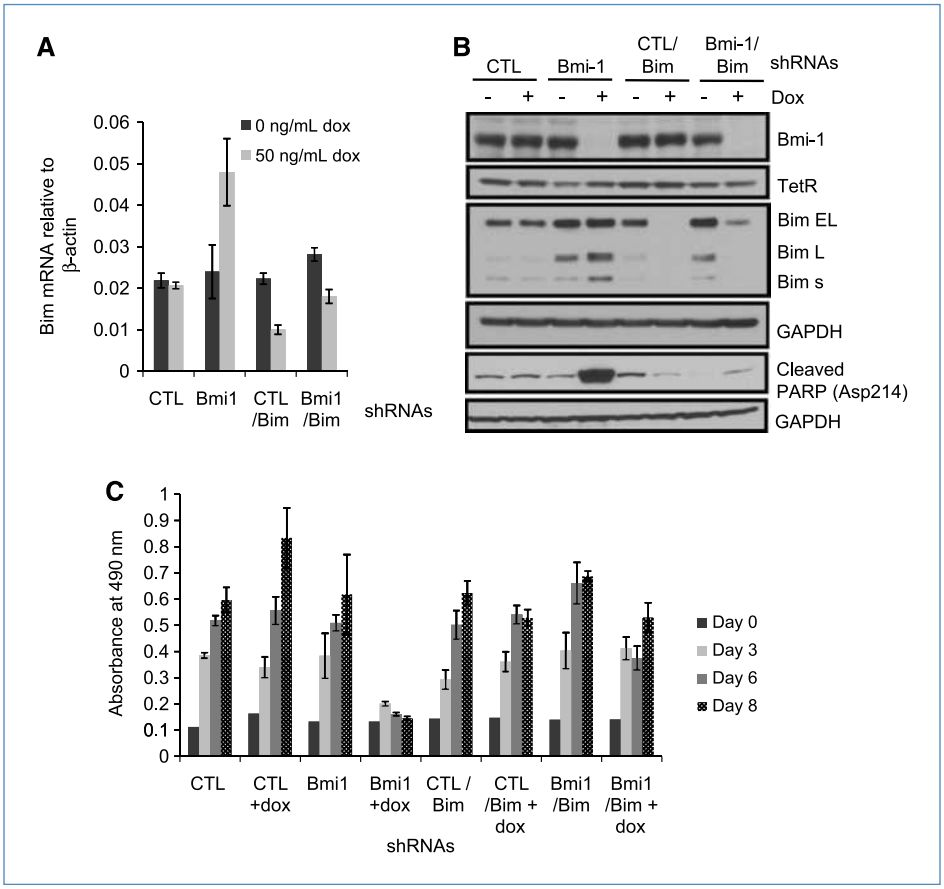

Figure 6. Bim knockdown rescues inhibition of growth induced upon Bmi-1 knockdown. A, qRT-PCR showing relative levels of Bim mRNA after 72 h of doxycycline treatment in RPMI-8226 cells either containing Bmi-1 shRNA alone, or a combination of Bmi-1 and Bim shRNAs. B, immunoblot confirming knockdown of Bim protein in control shRNA/Bim shRNA and Bmi-1 shRNA/Bim shRNA doxycycline–treated RPMI-8226 cells. Cells were harvested 3 d after doxycycline induction. Cleaved PARP (Asp214) expression increases upon Bmi1 knockdown but is inhibited with dual Bmi-1 and Bim knockdown. C, Bmi-1 shRNA and Bmi-1/Bim shRNA RPMI-8226 cells were seeded in triplicate at 2,000 cells per well in a 96-well plate. Cells were treated with doxycycline, and growth was measured using the Cell Titer 96 Aqueous One Solution cell proliferation assay. $P < 0.05$ for doxycycline induction of both Bmi-1/Bim shRNAs at day 8 compared with doxycycline induction of Bmi-1 shRNA alone.

overcome c-Myc induction of p19 and apoptosis (5). Therefore, the tumor-promoting function of Bmi-1 has been proposed to be in part due to the inhibition of apoptosis. In our myeloma system, knockdown of Bmi-1 resulted in the potent induction of apoptosis in RPMI-8226 cells, as well as the increased production of cleaved caspase-3 in the corresponding xenograft model. However, we did not observe any changes in *p16* or *p14* (human ARF) mRNA, suggesting *INK4a/ARF*-independent Bmi-1 function(s). We therefore undertook a global transcriptional profiling approach to elucidate novel genes that are regulated by Bmi-1. Our analysis uncovered a major proapoptotic protein, Bim, to be upregulated upon Bmi-1 knockdown. The repression of Bim expression by Bmi-1 seems to occur through a mechanism that involves Bmi-1 localization at the *Bim* promoter as indicated by our ChIP studies. Strikingly, dual knockdown of Bmi-1 and Bim caused an almost complete rescue of cells from undergoing apoptosis. To date, this is the first study that functionally links Bmi-1 to the regulation of the proapoptotic gene Bim. Therefore, our results establish that the repression of Bim by Bmi-1 plays an important role toward the survival of MM cells, as provided by the RPMI-8226 cell line model. Given the considerable genetic heterogeneity within MM, our data suggest that Bmi-1 promotes MM growth through potentially distinct mechanisms because we did not observe a strong apoptotic phenotype upon Bmi-1 knockdown in KMS12BM or LP1 cells. These findings are partly in agreement with reports that LP1 cells lack expression of Bim (50). In future studies, the mechanisms of Bmi-1–driven growth in such cell lines will need to be elucidated.

Our findings about the suppression of Bim downstream of Bmi-1 are intriguing in light of several studies that implicate *INK4a/ARF*-independent mechanisms by which Bmi-1 affects tumorigenesis (19, 21). In addition, even in Bmi-1 knockout models, *INK4a/ARF* deficiency does not confer a complete rescue against the senescent and apoptotic phenotypes observed, again suggesting the presence of additional Bmi-1 targets (5, 6). Indeed, genome-wide studies in human embryonic fibroblasts have revealed that the PcG proteins regulate the expression of various genes involved in differentiation and stem cell maintenance, some of which belong to the Wnt and Notch signaling pathways (51). As such pathways are deregulated in several cancers including MM, whether these targets are similarly regulated by the PcG proteins in the tumorigenic context and specifically in MM will be of interest to investigate in future studies.

In conclusion, we present evidence for the involvement of Bmi-1 function in MM as well as characterize a novel pathway by which Bmi-1 functions in inhibiting apoptosis. An understanding of Bmi-1–regulated pathways in normal as well as in the tumorigenic context will be crucial toward evaluating it as a potential target in anticancer therapy.

Disclosure of Potential Conflicts of Interest

Z. Jagani, D. Wiederschain, A. Loo, D. He, R. Mosher, P. Fordijour, J. Monahan, M. Morrissey, Y-M. Yao, M. Warmuth, W.R. Sellers, and M. Dorsch are employees of Novartis Institutes for BioMedical Research. C. Lengauer was a previous employee of Novartis Institutes for BioMedical Research, and is currently an employee of sanofi-aventis.

Acknowledgments

We thank Frank Stegmeier, Raymond Pagliarini, Ramesh Shivdasani, and William Matsui for critical advice; Kristy Chung for the assistance; and Shilpa Kadam, Felix Lohmann, David Ciccone, and Gilles Buchwalter for the advice on ChIP experiments.

The costs of publication of this article were defrayed in part by the payment of page charges. This article must therefore be hereby marked *advertisement* in accordance with 18 U.S.C. Section 1734 solely to indicate this fact.

Received 11/18/2009; revised 03/30/2010; accepted 04/16/2010; published OnlineFirst 06/08/2010.

References

1. van Lohuizen M, Verbeek S, Scheijen B, Wientjens E, van der Gulden H, Berns A. Identification of cooperating oncogenes in E mu-myc transgenic mice by provirus tagging. Cell 1991;65:737–52.
2. Haupt Y, Alexander WS, Barri G, Klinken SP, Adams JM. Novel zinc finger gene implicated as myc collaborator by retrovirally accelerated lymphomagenesis in E mu-myc transgenic mice. Cell 1991; 65:753–63.
3. van Lohuizen M, Frasch M, Wientjens E, Berns A. Sequence similarity between the mammalian bmi-1 proto-oncogene and the Drosophila regulatory genes Psc and Su(z)2. Nature 1991;353:353–5.
4. Schwartz YB, Pirrotta V. Polycomb silencing mechanisms and the management of genomic programmes. Nat Rev Genet 2007;8:9–22.
5. Jacobs JJ, Scheijen B, Voncken JW, Kieboom K, Berns A, van Lohuizen M. Bmi-1 collaborates with c-Myc in tumorigenesis by inhibiting c-Myc-induced apoptosis via INK4a/ARF. Genes Dev 1999; 13:2678–90.
6. Jacobs JJ, Kieboom K, Marino S, DePinho RA, van Lohuizen M. The oncogene and Polycomb-group gene bmi-1 regulates cell proliferation and senescence through the ink4a locus. Nature 1999; 397:164–8.
7. Bracken AP, Kleine-Kohlbrecher D, Dietrich N, et al. The Polycomb group proteins bind throughout the INK4A-ARF locus and are disassociated in senescent cells. Genes Dev 2007;21:525–30.
8. Leung C, Lingbeek M, Shakhova O, et al. Bmi1 is essential for cerebellar development and is overexpressed in human medulloblastomas. Nature 2004;428:337–41.
9. Vonlanthen S, Heighway J, Altermatt HJ, et al. The bmi-1 oncoprotein is differentially expressed in non-small cell lung cancer and correlates with INK4A-ARF locus expression. Br J Cancer 2001;84:1372–6.
10. Kim JH, Yoon SY, Jeong SH, et al. Overexpression of Bmi-1 oncoprotein correlates with axillary lymph node metastases in invasive ductal breast cancer. Breast 2004;13:383–8.
11. Berezovska OP, Glinskii AB, Yang Z, Li XM, Hoffman RM, Glinsky GV. Essential role for activation of the Polycomb group (PcG) protein chromatin silencing pathway in metastatic prostate cancer. Cell Cycle 2006;5:1886–901.
12. De Vos J, Thykjaer T, Tarte K, et al. Comparison of gene expression profiling between malignant and normal plasma cells with oligonucleotide arrays. Oncogene 2002;21:6848–57.
13. Chng WJ, Kumar S, Vanwier S, et al. Molecular dissection of hyperdiploid multiple myeloma by gene expression profiling. Cancer Res 2007;67:2982–9.
14. Zhan F, Barlogie B, Arzoumanian V, et al. Gene-expression signature of benign monoclonal gammopathy evident in multiple myeloma is linked to good prognosis. Blood 2007;109:1692–700.
15. Glinsky GV, Berezovska O, Glinskii AB. Microarray analysis identifies a death-from-cancer signature predicting therapy failure in patients with multiple types of cancer. J Clin Invest 2005;115:1503–21.

16. Glinsky GV. Death-from-cancer signatures and stem cell contribution to metastatic cancer. Cell Cycle 2005;4:1171–5.
17. Dovey JS, Zacharek SJ, Kim CF, Lees JA. Bmi1 is critical for lung tumorigenesis and bronchioalveolar stem cell expansion. Proc Natl Acad Sci U S A 2008;105:11857–62.
18. Michael LE, Westerman BA, Ermilov AN, et al. Bmi1 is required for Hedgehog pathway-driven medulloblastoma expansion. Neoplasia 2008;10:1343–9, 1345p following 1349.
19. Bruggeman SW, Hulsman D, Tanger E, et al. Bmi1 controls tumor development in an Ink4a/Arf-independent manner in a mouse model for glioma. Cancer Cell 2007;12:328–41.
20. Wiederschain D, Chen L, Johnson B, et al. Contribution of polycomb homologues Bmi-1 and Mel-18 to medulloblastoma pathogenesis. Mol Cell Biol 2007;27:4968–79.
21. Douglas D, Hsu JH, Hung L, et al. BMI-1 promotes ewing sarcoma tumorigenicity independent of CDKN2A repression. Cancer Res 2008;68:6507–15.
22. Lessard J, Sauvageau G. Bmi-1 determines the proliferative capacity of normal and leukaemic stem cells. Nature 2003;423:255–60.
23. Park IK, Qian D, Kiel M, et al. Bmi-1 is required for maintenance of adult self-renewing haematopoietic stem cells. Nature 2003;423:302–5.
24. Molofsky AV, Pardal R, Iwashita T, Park IK, Clarke MF, Morrison SJ. Bmi-1 dependence distinguishes neural stem cell self-renewal from progenitor proliferation. Nature 2003;425:962–7.
25. Liu S, Dontu G, Mantle ID, et al. Hedgehog signaling and Bmi-1 regulate self-renewal of normal and malignant human mammary stem cells. Cancer Res 2006;66:6063–71.
26. Seidl S, Kaufmann H, Drach J. New insights into the pathophysiology of multiple myeloma. Lancet Oncol 2003;4:557–64.
27. Richardson PG, Mitsiades C, Schlossman R, Munshi N, Anderson K. New drugs for myeloma. Oncologist 2007;12:664–89.
28. Wiederschain D, Wee S, Chen L, et al. Single-vector inducible lentiviral RNAi system for oncology target validation. Cell Cycle 2009;8:498–504.
29. Huang S, Sinicrope FA. BH3 mimetic ABT-737 potentiates TRAIL-mediated apoptotic signaling by unsequestering Bim and Bak in human pancreatic cancer cells. Cancer Res 2008;68:2944–51.
30. Wee S, Jagani Z, Xiang KX, et al. PI3K pathway activation mediates resistance to MEK inhibitors in KRAS mutant cancers. Cancer Res 2009;69:4286–93.
31. Hubbell E, Liu WM, Mei R. Robust estimators for expression analysis. Bioinformatics 2002;18:1585–92.
32. Hochberg Y, Benjamini Y. More powerful procedures for multiple significance testing. Stat Med 1990;9:811–8.
33. O'Connor L, Strasser A, O'Reilly LA, et al. Bim: a novel member of the Bcl-2 family that promotes apoptosis. EMBO J 1998;17:384–95.
34. Chiu R, Novikov L, Mukherjee S, Shields D. A caspase cleavage fragment of p115 induces fragmentation of the Golgi apparatus and apoptosis. J Cell Biol 2002;159:637–48.
35. Brancolini C, Benedetti M, Schneider C. Microfilament reorganization during apoptosis: the role of Gas2, a possible substrate for ICE-like proteases. EMBO J 1995;14:5179–90.
36. Wang L, Gao X, Gao P, et al. Cell-based screening and validation of human novel genes associated with cell viability. J Biomol Screen 2006;11:369–76.
37. Bouillet P, Huang DC, O'Reilly LA, et al. The role of the pro-apoptotic Bcl-2 family member bim in physiological cell death. Ann N Y Acad Sci 2000;926:83–9.
38. Tewari M, Yu M, Ross B, Dean C, Giordano A, Rubin R. AAC-11, a novel cDNA that inhibits apoptosis after growth factor withdrawal. Cancer Res 1997;57:4063–9.
39. Houde N, Chamoux E, Bisson M, Roux S. Transforming Growth Factor-{β}1 (TGF-{β}1) induces human osteoclast apoptosis by up-regulating Bim. J Biol Chem 2009;284:23397–404.
40. Cragg MS, Kuroda J, Puthalakath H, Huang DC, Strasser A. Gefitinib-induced killing of NSCLC cell lines expressing mutant EGFR requires BIM and can be enhanced by BH3 mimetics. PLoS Med 2007;4:1681–9; discussion 1690.
41. Shah NP, Kasap C, Weier C, et al. Transient potent BCR-ABL inhibition is sufficient to commit chronic myeloid leukemia cells irreversibly to apoptosis. Cancer Cell 2008;14:485–93.
42. Woo CJ, Kharchenko PV, Daheron L, Park PJ, Kingston RE. A region of the human HOXD cluster that confers polycomb-group responsiveness. Cell 140:99–110.
43. Bommert K, Bargou RC, Stuhmer T. Signalling and survival pathways in multiple myeloma. Eur J Cancer 2006;42:1574–80.
44. Podar K, Chauhan D, Anderson KC. Bone marrow microenvironment and the identification of new targets for myeloma therapy. Leukemia 2009;23:10–24.
45. Sparmann A, van Lohuizen M. Polycomb silencers control cell fate, development and cancer. Nat Rev Cancer 2006;6:846–56.
46. Alkema MJ, Jacobs H, van Lohuizen M, Berns A. Pertubation of B and T cell development and predisposition to lymphomagenesis in Emu Bmi1 transgenic mice require the Bmi1 RING finger. Oncogene 1997;15:899–910.
47. Datta S, Hoenerhoff MJ, Bommi P, et al. Bmi-1 cooperates with H-Ras to transform human mammary epithelial cells via dysregulation of multiple growth-regulatory pathways. Cancer Res 2007;67:10286–95.
48. Hoenerhoff MJ, Chu I, Barkan D, et al. BMI1 cooperates with H-RAS to induce an aggressive breast cancer phenotype with brain metastases. Oncogene 2009;28:3022–32.
49. Guo WJ, Datta S, Band V, Dimri GP. Mel-18, a polycomb group protein, regulates cell proliferation and senescence via transcriptional repression of Bmi-1 and c-Myc oncoproteins. Mol Biol Cell 2007;18:536–46.
50. Trudel S, Stewart AK, Li Z, et al. The Bcl-2 family protein inhibitor, ABT-737, has substantial antimyeloma activity and shows synergistic effect with dexamethasone and melphalan. Clin Cancer Res 2007;13:621–9.
51. Bracken AP, Dietrich N, Pasini D, Hansen KH, Helin K. Genome-wide mapping of Polycomb target genes unravels their roles in cell fate transitions. Genes Dev 2006;20:1123–36.